Cardiovascular response to orthostatic stress: multiscale modeling with focus on the coronary circulation

(Article begins on next page)

26 December 2024

CARDIOVASCULAR RESPONSE TO ORTHOSTATIC STRESS: MULTISCALE MODELING WITH FOCUS ON THE CORONARY CIRCULATION

Matteo Fois[1], Luca Ridolfi[2], and Stefania Scarsoglio[1]

[1]Department of Mechanical and Aerospace Engineering, Politecnico di Torino, 10129 Turin, Italy, {matteo.fois,stefania.scarsoglio}@polito.it

[2]Department of Environmental, Land and Infrastructure Engineering, Politecnico di Torino, 10129 Turin, Italy, luca.ridolfi@polito.it

SUMMARY

Cardiovascular modeling has shown impressive potentialities in understanding and predicting cardiovascular system (CVS) functioning, disorders and response under several conditions. By adopting a recent closed-loop multiscale model of the entire CVS, we computationally investigated the coronary hemodynamics response to passive orthostatic stress elicited by upright head-up tilt (HUT). Beside known CVS consequences following passive upright tilting – such as heart rate and blood pressure augmentation, stroke volume and cardiac output drop – we found that coronary blood flow (CBF) was enhanced by up to 18% at 70° HUT, in response to a coronary perfusion pressure (CPP) rise of 26%.

Key words: *coronary hemodynamics, head-up tilt test, computational hemodynamics, multiscale cardiovascular modeling*

1 INTRODUCTION

Even though the human cardiovascular system (CVS) response to passive change of posture (e.g., via head-up tilting) has been extensively explored [1, 2], the detailed description of the hemodynamics alterations involving specific vasculature - such as the coronary circulation - still lacks full comprehension [3]. To date, little is known regarding the effect of passive orthostatic stress onto perfusion of the myocardium [4]. In this perspective, numerical modeling can be exploited as diagnostic and prognostic tool to explore the CVS response under several physiological and pathological conditions [5, 6, 7].

In our analysis, we employed the closed-loop model of the CVS developed in our recent work [8] to investigate the coronary hemodynamics response to simulated head-up tilt (HUT) from supine to 70°. Beside the typical hemodynamic parameters alteration - including heart rate (HR), stroke volume (SV), cardiac output (CO) and total peripheral resistance (TPR) - triggered by orthostatic stress, we focused on the behavior of the most relevant coronary hemodynamics parameters, such as coronary perfusion pressure (CPP) and coronary blood flow (CBF). Further observations were conducted concerning left and right main coronary arteries blood flow unbalance, the different myocardial layers perfusion and the coronary vascular resistance behavior.

2 METHODOLOGY

The closed-loop multiscale architecture of the model (see Figure 1) is composed of a 1D description of the arterial tree, linked to 0D analogs of the systemic peripheral circulation, microcirculation, venous return and cardiopulmonary circulation. The detailed description of the mathematical model of the CVS is provided in our recent work [8].

Blood motion through large arteries is governed by the 1D axisymmetric form of mass and momentum balance equations (eqs. A and B in Figure 1), where variables $A(x,t)$ and $Q(x,t)$ denote vessel
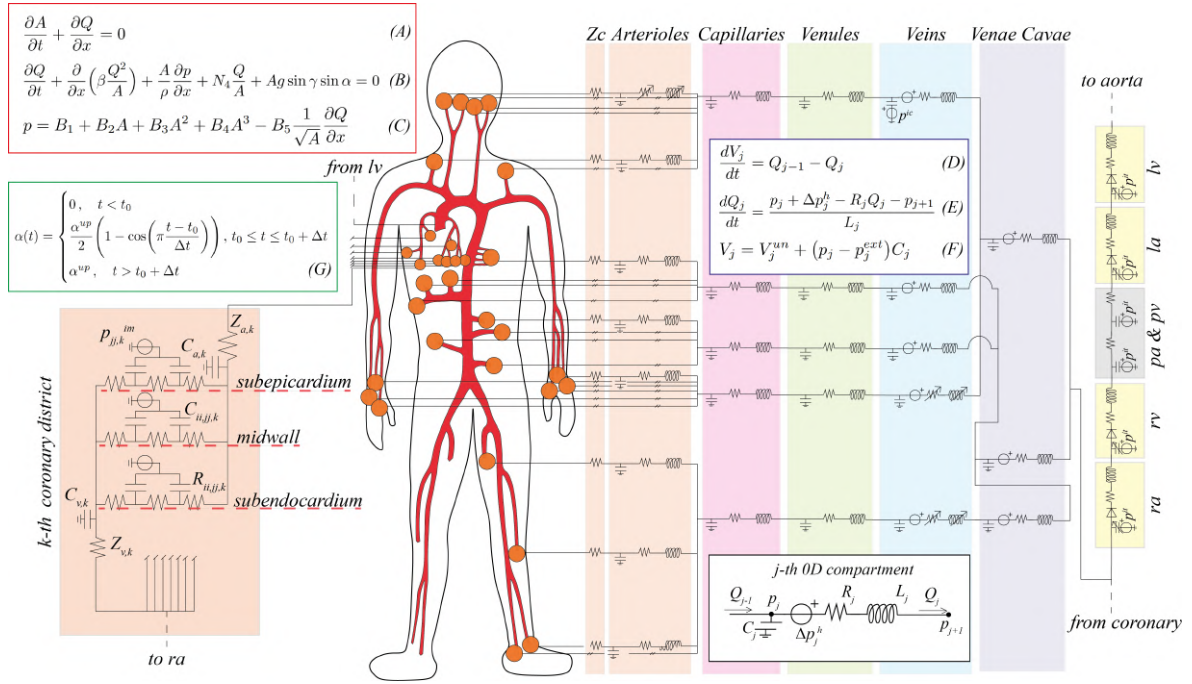
Figure 1: schematic illustration of the global multiscale CVS model. The red network illustrates the 1D arterial tree, whereas the right coloured boxes (from orange to blue) depicts the systemic 0D compartments. The orange circles represent the connection between 1D and 0D models at distal arterioles. The orange box on the left illustrates the k-th 0D coronary microcirculatory district, while the generic j-th 0D systemic compartment is displayed in the bottom box. Z_c are characteristic impedances. The model equations are reported in the red, blue and green boxes, indexed from A to G. Cardiac chambers are denoted as ra, rv, la and lv; pulmonary arteries and veins are indicated as pa and pv, respectively.

cross-section area and blood flow rate, respectively (t is time and x the vessel axial coordinate, ρ is blood density, β is the Coriolis coefficient and N_4 is the viscous coefficient). Gravity is included through the term $g \sin \gamma \sin \alpha$, where g is the gravity acceleration, γ is the orientation of the vessel with respect to the frontal transverse body axis, and α is the tilt angle with respect to the horizontal reference. Blood pressure $p(x,t)$ is derived through a non-linear constitutive visco-elastic law of A and Q (eq. C reported in Figure 1), accounting for vessels geometry and walls mechanical properties (coefficients B_i, $i = 1 \ldots 5$). Systemic 0D compartments (arteriolar, capillary, venular, venous and venae cavae) are governed by equations D, E and F (Figure 1), where $Q_j(t)$, $p_j(t)$ and $V_j(t)$ are blood flow rate, intraluminal pressure and total volume, respectively. Δp_j^h, p_j^{ext} and V_j^{un} denote extravascular pressure, blood hydrostatic pressure and unstressed volume of the j-th compartment, respectively. R_j, C_j and L_j are the j-th compartmental lumped resistance, compliance and inertance, respectively; j indicates the current compartment, with $j \pm 1$ being the following/preceding compartment. Such compartments are organized into five separate body regions: head, arms, upper abdomen, lower abdomen and legs. The cardiopulmonary circulation is described by a time-varying elastance model and a valve model for each cardiac chamber, plus arterial and venous pulmonary 0D compartments.

The coronary circulation is based on the multiscale 1D-0D model developed by Mynard & Smolich [5] (see [7] for the coronary model calibration and mathematical details, including its coupling with the systemic circulation). Each 1D terminal coronary artery is attached to a 0D analog of the myocardial layers microcirculation, from subepicardium to subendocardium (refer to Figure 1). $Z_{a,k}$ and $Z_{v,k}$, are arterial and venous input/output impedances, $C_{a,k}$ and $C_{v,k}$ and arterial and venous input/output compliances, $C_{ii,jj,k}$ and $R_{ii,jj,k}$ are intra-layer compliances (constant) and resistances (time-varying according to the local blood volume). The term $p_{jj,k}^{im}$ is the intramyocardial pressure, determined by the periodic contraction of the adjacent ventricles: this behavior makes the coronary circulation peculiar allowing blood to flow mostly during heart diastole.

Autonomic regulation of blood pressure is achieved via the combined arterial baroreflex and cardiopulmonary reflex control. Furthermore, a cerebral autoregulation model is enclosed to mimic

RMCA	0°	70°	Δ
$\bar{Q}$ [ml/s]	1.10	1.33	+21%

LMCA	0°	70°	Δ
$\bar{Q}$ [ml/s]	3.37	3.95	+17%

LAD	0°	70°	Δ
$\bar{Q}$ [ml/s]	1.67	1.97	+18%

LCx	0°	70°	Δ
$\bar{Q}$ [ml/s]	1.71	1.98	+16%

ENDO,r	0°	70°	Δ
$\bar{Q}$ [ml/s]	0.14	0.16	+15%

EPI,r	0°	70°	Δ
$\bar{Q}$ [ml/s]	0.10	0.11	+15%

ENDO,l	0°	70°	Δ
$\bar{Q}$ [ml/s]	1.16	1.36	+18%

EPI,l	0°	70°	Δ
$\bar{Q}$ [ml/s]	0.89	1.05	+18%

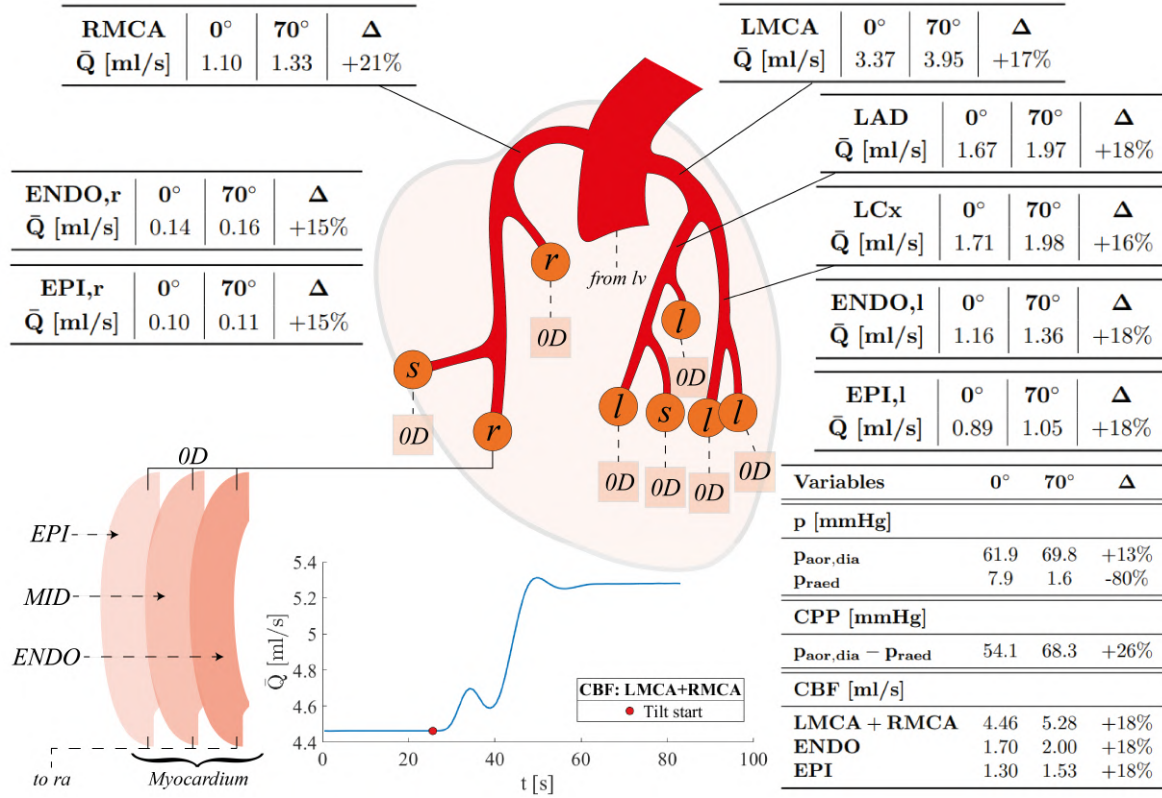| Variables	0°	70°	Δ
p [mmHg]			
$p_{aor,dia}$	61.9	69.8	+13%
p_{raed}	7.9	1.6	-80%
CPP [mmHg]			
$p_{aor,dia} - p_{raed}$	54.1	68.3	+26%
CBF [ml/s]			
LMCA + RMCA	4.46	5.28	+18%
ENDO	1.70	2.00	+18%
EPI	1.30	1.53	+18%

Figure 2: schematic illustration of the coronary hemodynamics response to passive HUT. LMCA and RMCA denote left main and right main coronary arteries, respectively, LAD and LCx are the left anterior descending and left circumflex arteries, EPI, MID and ENDO indicate the subepicardial, midwall and subendocardial mirocirculatory layers of the myocardium, respectively (total ENDO and EPI CBF were calculated collecting blood flow through the related myocardial layer of all 0D districts, whereas suffixes l and r refer to arteries perfusing left and right heart, respectively; s denotes septal arteries). $\bar{Q}$ is beat-to-beat mean blood flow rate, $p_{aor,dia}$ and p_{raed} are aortic diastolic pressure and right atrium end-diastolic pressure, respectively.

cerebral blood flow conservation. The model reproduces also venous valves intervention within the arms and legs compartments, and the action of intracranial and intrathoracic pressures (p^{ic}, p^{it} in Figure 1) onto head venous and thoracic compartments.

HUT tests are simulated according to Heldt [6], by varying the tilt angle $\alpha(t)$ as a cosinusoidal function of time (see eq. G in Figure 1, where $\alpha^{up} = 70°$, while t_0 and $\Delta t = 17.5s$ ($4°/s$) are tilt starting time and duration, respectively).

3   RESULTS AND CONCLUSIONS

The model was employed to analyze the steady-state and transient response of the CVS to passive HUT. The main hemodynamics alterations following posture changes to different degree of tilt (widely documented in the literature [1, 3, 2]) included HR (+25%), central arterial pressure (diastolic pressure +14%) and TPR (+39%) increase accompanied by SV (-33%), CO (-19%) and central venous pressure (CVP, -80%) drop (results at 70° HUT, see [8]). Here, we focused on the coronary circulation, whose behavior during passive HUT was barely investigated so far, according to the authors knowledge.

Figure 2 displays the most relevant hemodynamic alterations registered within the coronary vasculature upon passive tilting to 70°. By evaluating CPP as the difference between aortic diastolic pressure ($p_{aor,dia}$, raised by about 8 mmHg after tilting to 70°) and right atrium end-diastolic pressure (p_{raed}, dropped from 7.9 mmHg to 1.6 mmHg), we found that it increased by +26% with respect to supine posture (bottom right table in Figure 2). Being the main coronary driving pressure, CPP can be considered as a proxy of CBF. The latter was then computed directly during the tilting simulation as the

summation of the beat-to-beat mean flow rate $\bar{\mathbf{Q}}$ through the LMCA and the RMCA (blue line in the bottom diagram of Figure 2). Despite the upstream reduction in systemic SV and CO, a noticeable increase in LMCA+RMCA blood flow from 4.46 ml/s to 5.28 ml/s (+18%, bottom right table in Figure 2) was registered after tilting. The rise in CPP and CBF can be explained by the contraction of the systemic pulse pressure (mainly due to the augmented diastolic pressure) along with the drop in intrathoracic pressure (linked to the decreased p_{raed}, as well as all cardiac pressures) and the reduced right atrial filling driven by blood shift to lower extremities. The coronary vascular resistance $\mathbf{R_{cor,eq}}$ was approximated as the equivalent resistance of all the 0D microcirculatory districts. No significant variation was detected for this quantity between supine and 70° upright, since almost no blood migration occurred after tilting (coronary vascular resistance depends on the inverse of coronary blood volume squared).

In addition, due to $\mathbf{R_{cor,eq}}$ invariance, almost no difference in CBF emerged from an inter-layer point of view: +18% in total subendocardial (ENDO) and +18% in total subepicardial (EPI) vessels (summed over all 0D districts), between supine and 70° upright, as reported in the bottom right table of Figure 2 and in the small tables on the right and left sides of Figure 2 (+18% for both ENDO,l and EPI,l; +15% for both ENDO,r and EPI,r). From a left-to-right perspective instead, a little unbalance was revealed towards right coronary arteries (+21% at RMCA, in the small table on top left side of Figure 2) with respect to left coronary arteries (+17% at LMCA, +18% and +16% at LAD and LCx coronary arteries, in the small tables on top right side of Figure 2). A potential reason for such unbalance may be found in the different intra-chamber pressure of the adjacent ventricle, leading to higher left coronary arteries flow obstruction with respect to right heart.

In conclusion, our analysis showed that passive upright posture enhances CBF likely because of the augmented CPP. Our results are qualitatively in agreement with those by van Lieshout et al. [4]), since only indirect measurements of CBF variation following changes of posture were reported in their work. We acknowledge that our model lacks of additional coronary autoregulation mechanisms - such as metabolic and myogenic CBF regulation - beside passive adjustment of vascular resistance. These mechanisms would probably limit CBF increment caused by HUT-induced CPP and HR rise, although their interplay with post-tilt reduced oxygen consumption revealed in our previous work [8] suggests that further investigation is needed.

REFERENCES

[1] T. Coonan and C. Hope. Cardio-respiratory effects of change of body position. *Canadian Anaesthetists' Society Journal*. 30: 424–437, 1983. DOI: 10.1007/BF03007869.

[2] K. Toska, and L. Walløe. Dynamic time course of hemodynamic responses after passive head-up tilt and tilt back to supine position. *Journal of Applied Physiology*. 92: 1671—1676, 2002. DOI: 10.1152/japplphysiol.00465.2000.

[3] C.G. Blomqvist and H.L. Stone. (1991). Cardiovascular adjustments to gravitational stress. *Comprehensive Physiology*. 1025–1063, 2011. DOI: 10.1002/cphy.cp020328.

[4] J. Van Lieshout, M. Harms, F. Pott, M. Jenstrup, and N. Secher. Stroke volume of the heart and thoracic fluid content during head-up and head-down tilt in humans. *Acta anaesthesiologica scandinavica*. 49:1287—1292, 2005. DOI: 10.1111/j.1399-6576.2005.00841.x.

[5] J.P. Mynard and J.J. Smolich. One-dimensional haemodynamic modeling and wave dynamics in the entire adult circulation. *Annals of biomedical engineering*, 43:1443–1460, 2015. DOI: 10.1007/s10439-015-1313-8.

[6] T. Heldt. Computational models of cardiovascular response to orthostatic stress. *Massachusetts Institute of Technology*, 2004. DOI: http://hdl.handle.net/1721.1/28761.

[7] A. Saglietto, M. Fois, L. Ridolfi, G.M. De Ferrari, M. Anselmino and S. Scarsoglio. A computational analysis of atrial fibrillation effects on coronary perfusion across the different myocardial layers. *Scientific Reports*, 12:841, 2022. DOI: 10.1038/s41598-022-04897-6.

[8] M. Fois, S.V. Maule, M. Giudici, M. Valente, L. Ridolfi and S. Scarsoglio. Cardiovascular response to posture changes: multiscale modeling and in-vivo validation during head-up tilt. *Frontiers in Physiology*, 13, 2022. DOI: 10.3389/fphys.2022.826989.